A selective fluorescent 'turn-on' sensor for recognition of Zn^{2+} in aqueous media

Mecit Ozdemir

PII: S1386-1425(16)30097-X
DOI: doi: 10.1016/j.saa.2016.02.040
Reference: SAA 14306

To appear in:

Received date: 14 September 2015
Revised date: 20 February 2016
Accepted date: 28 February 2016

Please cite this article as: Mecit Ozdemir, A selective fluorescent 'turn-on' sensor for recognition of Zn^{2+} in aqueous media, (2016), doi: 10.1016/j.saa.2016.02.040

A selective fluorescent 'turn-on' sensor for recognition of Zn^{2+} in aqueous media

Mecit Ozdemir[a*]

Department of Food Processing, Vocational High School, Kilis 7 Aralik University, Kilis, Turkey

* Corresponding author. Tel.: +90 348 814 26 62; fax: +90 348 814 26 63.

E-mail address: mecitozdemir@kilis.edu.tr

ABSTRACT

A new rhodamine-based fluorescent probe '**RhAP**' was synthesized and successfully characterised using FT-IR, ^{13}C NMR, ^{1}H NMR spectroscopies, LC-MS/MS spectrometry and elemental analysis. The **RhAP**, a colorless and non-fluorescent compound, showed a selective fluorescent response and colorimetric change for Zn^{2+} in HEPES buffered (10 mM, EtOH:water, 2:1, v/v, pH 7.2). Upon the addition of two equivalents of Zn^{2+} to a solution of **RhAP**, a nearly 35-fold enhancement of the fluorescence intensity, with an emission maximum at 578 nm, was observed in comparison to the sensor alone under the same experimental conditions. The complex formation between **RhAP** and Zn^{2+} was found to have a 1:1 ratio based on calculations obtained from the Job's plot and the mole ratio plot methods. The results showed that **RhAP** can be used as an effective fluorescent probe for selective detecting of Zn^{2+} in an aqueous medium.

Keywords: Fluorescent sensor, rhodamine, selective, colorimetric, zinc

1. Introduction

In recent years, researchers have become increasingly interested in the design and development of fluorescent sensors based on ion-induced changes in fluorescence due to these sensors' highly selective and sensitive recognition of biologically and environmentally crucial heavy and transition metal (HTM) ions, and their ability to sense and identify many special metal species [1]. Zinc is the second most abundant transition metal ion in the human body with concentrations ranging from nanomolar (nM) to millimolar (mM) [2]. And also, it is an important cofactor in many biological processes such as neural-signal transmissions and pathology, the regulation of metalloenzymes, gene transcription, immune function, and mammalian reproduction. In addition, the disorder of zinc metabolism in biological systems has been correlated to epilepsy, diabetes, infantile diarrhoea and Alzheimer's disease [3]. From this perspective, the detection of heavy metal ions based on a highly selective and sensitive fluorescent chemosensor in aquatic ecosystems, drinking water and biological systems is still a significant research topic due to the serious health issues these ions pose [4]. Although a number of chemosensors for the detection of zinc have been presently investigated, novel fluorescent 'turn-on' probes, which are capable of selectively detecting the presence of zinc ions in biological and environmental system in aqueous medium under physiological pH conditions, are still a considerable demand [5]. Therefore, chemists, biologists, clinical biochemists and environmentalists have recently expressed an interest in the need to design and develop synthetic receptors that are capable of recognising biologically and environmentally important ion species. Thus, fluorescent probes that have a turn-on increase or ratiometric response to Zn^{2+} are increasingly receiving a great deal of attention, and demand for them is still high [6-9].

As we well known, rhodamine B and its derivatives have commonly been used as an important class of fluorogenic and chromogenic sensors to visualise metal ions in living cells without causing cell damage because of their unique properties such as high fluorescence quantum yields, good photostability, simplicity, low detection limit (LOD), capability for special recognition and other excellent spectroscopic properties [10]. Rhodamine based chemosensors are generally non-fluorescent and colorless. However, upon binding with the cation, the ring-open form of the rhodamine moiety leads to not only strong absorbance and fluorescence intensity changes, but also it shows an obvious color change during the sensing event, providing "naked-eye" detection [11-12].

Herein, we introduce a novel, selective fluorescent turn-on sensor rhodamine-based fluorescent probe '**RhAP**' based on the metal-coordination induced fluorescent activation (CIFA) mechanism. The **RhAP** chemosensor was prepared from a derivative of rhodamine B, which has a xanthene fluorophore in a spiro-ring configuration. According to the previous reports, the spirolactam moiety of the sensor prepared from a rhodamine derivative is expected to act as a signal switcher, which is visualized to turn on upon binding with metal cations [5, 13-15]. Consequently, the proposed **RhAP** chemosensor displayed a selective fluorescent response and visible change from colorless to purple. Fluorescence spectroscopic study of the sensor's interaction with Zn^{2+} also showed that **RhAP** is highly selective toward zinc more so than other competing metal ions under identical conditions.

2. Experimental Procedure

2.1. Equipment and reagents

Unless otherwise specified, chemicals were purchased from commercial suppliers and used without further purification. 2-Acetylpyridine and metal salts (nitrate or chloride) were purchased from Sigma-Aldrich and Merck. All the solvents were of analytic grade and water was redistilled. Rhodamine hydrazine was synthesized according to the method outlined in a previous report [16]. Structural characterization of the **RhAP** was carried out using Fourier transform infrared (FT-IR), hydrogen-1 nuclear magnetic resonance (^{1}H NMR), carbon-13 nuclear magnetic resonance (^{13}C NMR), liquid chromatography–mass spectrometry (LC-MS/MS), elemental analyses, fluorescence spectra and UV-Vis spectra techniques. The ^{1}H NMR and ^{13}C NMR spectra were recorded on a Bruker AVANCE III HD 400 NMR spectrometer using deuterated chloroform ($CDCl_{3)}$ as the solvent and tetramethylsilane (TMS) as an internal standard. LC-MS/MS analyses were conducted using a Varian 325-MS detection system. FT-IR spectra were measured using a PerkinElmer Spectrum 100 spectrometer. Absorption spectra were measured using a Varian Cary 100 Bio spectrophotometer at 298 K. All fluorescent measurements were conducted using a Varian Cary eclipse fluorescence spectrophotometer at 298 K. The pH measurements were determined using a Corning pH meter equipped with a Sigma-Aldrich micro combination electrode calibrated with a standard buffer solution.

To prepare the stock solutions of metal ions, the nitrate or chloride salts, Na^{+}, K^{+}, Ca^{2+}, Mg^{2+}, Cr^{3+}, Fe^{3+}, Hg^{2+}, Cu^{2+}, Pb^{2+}, Zn^{2+}, Fe^{2+}, Co^{2+}, Ni^{2+}, Cd^{2+}, Al^{3+}, Mn^{2+} and Ag^{+}, were

dissolved in double-distilled water to create 1 mM aqueous solutions. A 1 mM stock solution of **RhAP** was prepared in EtOH. These solutions were further diluted to the micro-molar (μM) level for fluorescence and absorption spectroscopy measurements with an EtOH-water (2:1, v:v) buffer (10 mM, HEPES, pH 7.2). Although the stock solution of **RhAP** used in the experimental studies was stored for more than one month under daylight conditions, no changes in spectroscopic properties were observed.

*2.2. Synthesis of **RhAP***

The **RhAP** was synthesized using the procedures previously reported in [17]. In short, 2-acetyl-pyridine (242 mg, 2 mmol) in ethanol, with a few drops of acetic acid, was slowly added to the ethanolic solution of rhodamine hydrazide (912 mg, 2 mmol). The mixture was stirred and heated to reflux overnight. The crude product evaporated under the reduced pressure and the mixture was purified by silica gel column chromatography using CH_2Cl_2/CH_3OH (20:1, v/v) as the eluent to afford a 0.86 g pure product, a 76 % yield of colorless **RhAP**.

Elemental Anal. (Calcd./Found): % C (74.97/74.68), % H (6.28/6.32), % N (12.87/12.80). FT-IR (**RhAP**, ν/cm^{-1}): 3084(vw, ν_{Ar-H}), 2967-2923(w, ν_{C-H}), 1691(vs, $\nu_{C=O}$); 1614(vs, $\nu_{C=N}$, azomethine), 1548(m, Py, $\nu_{C=N}$), 1514(vs, Ar, $\nu_{C=C}$), 1426, 1304, 1216, 1116(C-O); 1079, 815, 785, 755, 698, 674, 569, 531(Supplemental Fig. S1). FT-IR (**RhAP**+Zn^{2+}, ν/cm^{-1}): 3086 (vw, ν_{Ar-H}), 2973-2930(w, ν_{C-H}), 1645(w, $\nu_{C=O}$), 1586(vs, $\nu_{C=N}$, azomethine), 1508(w, Py, $\nu_{C=N}$), 1466(m, Ar, $\nu_{C=C}$), 1466, 1411, 1335, 1272, 1246, 1180, 1011, 922, 821, 785, 683, 496 (Supplemental Fig. S2). ^{1}H NMR ($CDCl_3$-*d*, 400 MHz) δ(pmm): 8.52(d, 1H), 7.8(d, 1H), 7.5(t, 2H), 7.48(m, 2H), 7.19(d, 2H), 6.59(d, 2H), 6.3(s, 2H), 6.28(d, 2H), 3.33(q, 8H), 2.37(s, 3H), 1.15(t, 12H)(Supplemental Fig. S3). ^{13}C NMR ($CDCl_3$-*d*, 400 MHz**)** δ(pmm)**:** 169(**C**17), 161(**C**24), 160, 159, 155, 153,151, 148, 144, 136, 132, 131, 128, 124, 123, 122, 108, 106, 97, 77(solvent), 44,5(**C**34,35,39,40), 17,51(**C**25), 12,86(**C**35,37,41,42) (Supplemental Fig. S4). ESI-MS: The mass spectrum of the chemosensor was represented in Supplemental Fig. S5. Fragments at m/z = 582 (base peak) was attributed to molecular ion peak $[C_{35}H_{37}N_5O_2 + Na]^+$. The other one at m/z = 560 appeared in the mass spectra was attributed to $[C_{35}H_{37}N_5O_2 + H]^+$. In addition to those peaks, there are also fragmentation products of molecular ion such as 423, 236, 183, and 101.

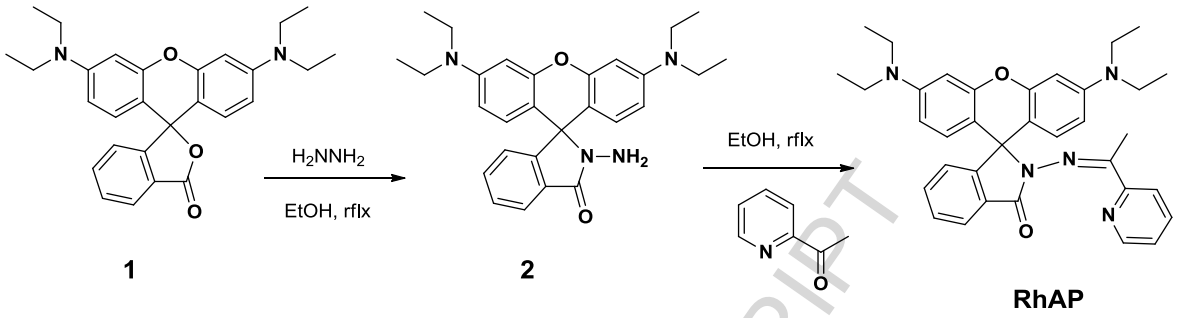

Scheme 1. Synthesis of the chemical probe **RhAP**

2.3. Determination of the binding mode (S:M), dissociation constant (K_d) and limit of detection (LOD)

The stoichiometry of **RhAP** with Zn^{2+} was determined using the Job's plot and the mole ratio plot methods. The absorption enhancement observed at 562 nm was plotted against the molar value of the [Zn^{2+}]/ [Zn^{2+}] + **RhAP** and [Zn^{2+}]/**RhAP**. The maximum absorption enhancements were obtained at 0.23 (Job's plot calculation) and 3.1 (mole ratio plot calculation). The dissociation constant of the **RhAP** sensor was determined using the Benesi-Hildebrand equation (Eq. 1) by employing fluorescence titration data. For the practical application, the LOD of the **RhAP** to Zn^{2+} was also calculated by using IUPAC equation [18].

3. Results and Discussion

The **RhAP** chemosensor was designed and prepared from rhodamine hydrazide and 2-acetylpyridine in ethanol, with a good yield. The compound was successfully characterised using elemental analysis, FT-IR, ^{1}H-NMR, ^{13}C-NMR and LC-MS/MS methods. All the characterization studies confirmed the structure of the **RhAP**, which is a colorless powder that is highly stable in ethanol. Moreover, the geometry of **RhAP** was optimised using the density functional theory (DFT) method with the 6-31G (d, p) basis set in the ground state. Molecular electrostatic potential (MEP) and frontier molecular orbitals (FMOs) of the fluorescent probe prepared in this study were investigated using theoretical calculations (Supplemental Figs. S6 and S7) [9, 19].

In order to better understand the fluorescent sensor's ability to distinguish between the sensor and the zinc ions in HEPES buffered (10 mM, EtOH:water, 2:1, v/v, pH 7.2), fluorescence and UV-vis spectroscopy techniques that were previously reported in the literature were used. The

stock solutions of the sensor and the metal ions were prepared at a concentration of 1 mM, and it was diluted to the micro-molar (μM) level [20-21].

3.1. Binding mode and sensing mechanism

According to the previously reported mechanism for some types of **RhAP** chemsensors, it is possible that the metal cations coordinate with the corresponding atom of the rhodamine group and cause the spirolactam ring to open [22-26]. This indicates that the carbonyl oxygen atom of spirolactam moiety plays an important role in binding **RhAP** to Zn^{2+} [27-30]. In order to shed some light on the binding mode for the complexation between **RhAP** and Zn^{2+}, IR and ^{1}H NMR spectra experiments were carried out, which indicated the coordination of the atoms (ONN) of receptor to zinc by opening of the spirolactam ring. IR spectra of **RhAP** and **RhAP**-Zn^{2+} were measured in ATR method, respectively, and the results were shown in Fig. 1. The characteristic stretching peaks at 1691.43 cm^{-1}, which corresponds to the carbonyl ($\nu_{C=O}$) absorption of **RhAP**, was shifted to a lower frequency (1645 cm^{-1}) upon chelating with Zn^{2+}, showing that a strong polarization of the C=O bond and also the cleavage of N-C bond in the spirolactam ring by the effective interaction of the **RhAP** with Zn^{2+}. Also, the stretching bands corresponding to the $\nu_{C=N}$ (azomethine) and $\nu_{C=N}$ (pyridine) in the **RhAP** were recorded at 1614.31 and 1548 cm^{-1}, respectively. Those of characteristic absorption bands of free **RhAP**, in cm^{-1}, were also shifted to lower wave numbers by 25 to 40 cm^{-1} on complexation. The IR spectrum of the **RhAP** + Zn^{2+} apparently gives evidence of coordination of the azomethine '*N'* and the pyridine '*N'* atoms and of the amidic carbonyl '*O*' atom [31-33].

Fig. 1

To further support the binding structure, ^{1}H NMR spectra of **RhAP** was recorded in the absence and presence of the 0.5 and 1.1 equiv. amount of the zinc salt dissolved in water, as depicted in the supplemental Fig. S8. In the ^{1}H NMR spectra, the signals of **RhAP** for the different types of assigned protons that are in the aromatic and aliphatic regions in the presence of zinc ions showed chemical shift changes. The **RhAP**-Zn^{2+} complex signal pattern of the aromatic and aliphatic protons also demonstrates the involvement of the pyridine moiety of the probe unit of **RhAP** in the binding of Zn^{2+}. According to these findings, a possible binding mode for **RhAP** with Zn^{2+} was proposed as presented in Scheme 2 [34-36].

Based on these determinations, the change in color can also be related to the structural transformation of **RhAP** from the spirolactam (non-fluorescent) form to the ring-opened (fluorescent) form owing to its complexation with Zn^{2+}. Thereby, as shown in Scheme 2 and Fig. 2, the colorless solution turned purple, which provided "naked-eye" detection of Zn^{2+} due to the ring opening of spirolactam of the sensor, when Zn^{2+} was added to the **RhAP** in the HEPES buffer solution. However, the addition of other competing metal ions did not lead to changes in the color of the **RhAP** solution in the absence of Zn^{2+}, except when the competing metal ions, Co^{2+}, Ni^{2+} and Cu^{2+} were present.

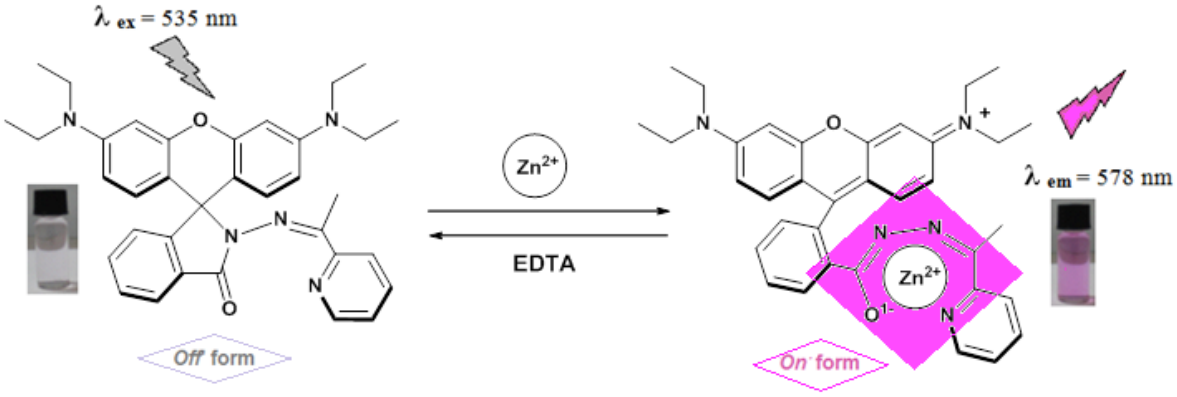

Scheme 2. The proposed binding mechanism of **RhAP** induced by Zn^{2+} in HEPES buffered (10 mM, EtOH:water, 2:1, v/v, pH 7.2). The insert shows the change of the color with the addition of Zn^{2+} to **RhAP** in buffered solution.

Figs. 2

3.2. Selectivity of the Sensor

To further investigate the cation binding properties of **RhAP**, its sensitivity was determined and selectivity studies for Zn^{2+} ions were conducted using UV-vis and fluorescence spectroscopy techniques with various possible interfering metal ions, as shown in Figs. 3 and 4. The absorption spectra of free **RhAP** in an EtOH-water solution displayed almost no absorption between 450 nm and 600 nm. Except for absorption increases for Zn^{2+}, Co^{2+}, Ni^{2+} and Cu^{2+}, other competing metal ions did not cause considerable absorption changes of **RhAP**, as presented in Fig. 3. This was attributed to the closed (spirolactam) forms of the sensor molecules in the solution. As depicted in Fig. 2, only Zn^{2+}, Co^{2+}, Ni^{2+} and Cu^{2+} induced a notable color change in the buffer solution under visible light, which can be ascribed to the spirolactam bond cleavage of the fluorophore

group, while the other metal ions did not show any obvious response [37-42]. Furthermore, the addition of Na^{+}, K^{+}, Ca^{2+}, Mg^{2+}, Cr^{3+}, Fe^{3+}, Al^{3+}, Mn^{2+}, Hg^{2+}, Cu^{2+}, Pb^{2+}, Fe^{2+}, Co^{2+}, Ni^{2+}, Cd^{+2} and Ag^{+} exerted little or no effect on the emission intensity of **RhAP**, while remarkable fluorescence enhancement was detected with the addition of Zn^{2+} by excitation of the fluorescent sensor at 535 nm. As depicted in Fig. 4, **RhAP** showed high fluorescence selectivity towards Zn^{2+} over the other metal ions, with the exception of a small amount of fluorescence enhancement for Fe^{2+} and Pb^{2+} (II). Meanwhile, when Co^{2+}, Ni^{2+} and Cu^{2+} ions were added to the sensor solution, significant changes in UV-vis spectra were observed. However, the fluorescence intensity did not increase when those metal ions were added because of their well-known paramagnetic properties. They have unfilled *d* shells, which might quench the fluorescence of sensor via electron or energy transfer [43-45].

To further explore the ability of probe **RhAP** to sense Zn^{2+}, fluorescence titration experiments on the sensor solution with Zn^{2+} were conducted in an EtOH-water solution under physiological pH conditions. As shown in Supplemental Fig. S9, the fluorescence intensity steadily increased when Zn^{2+} was progressively added to the **RhAP** solution. From the titration profiles, the dissociation constant ($\mathbf{K_d}$) and the LOD of **RhAP** for Zn^{2+} were determined.

Thanks to the fluorescence response of **RhAP** toward Zn^{2+} in the presence and absence of ions, such as Na^{+}, K^{+}, Ca^{2+}, Mg^{2+}, Ag^{1+}, Cr^{3+}, Fe^{3+}, Al^{3+}, Mn^{2+}, Hg^{2+}, Cu^{2+}, Pb^{2+}, Fe^{2+}, Co^{2+}, Ni^{2+} and Cd^{+2}, comparative experiments of zinc with various other metal ions were also conducted as given in Supplemental Fig. S10. The reduced selectivity for Zn^{2+} did not change with the addition of the other metal ions; only Fe (II) and Pb (II) showed a very small increase in fluorescence intensity. Furthermore, Supplemental Fig. S10 also reveals that some alkaline, alkaline-earth or transition metal ions do not interfere with the Zn^{2+}-induced fluorescence increase. This demonstrates that the proposed **RhAP** chemosensor has a good selectivity and sensitivity toward Zn^{2+}.

In addition, the reversibility of the fluorescent probe has been a significant aspect in practical applications. The coordination that occurs between **RhAP** and Zn^{2+} was found to be reversible using ethylenediamminetetraacetic acid (EDTA) titration, as supported in Fig. 5 and Scheme 2. Once the **RhAP**-Zn^{2+} complex was finally treated with 0.3 mM EDTA, the purple solution turned colorless, which confirmed that the coordination of this fluorescent probe with Zn^{2+} is reversible by chemical processes [33, 46].

Figs. 3, 4, and 5

3.3. The effect of pH on fluorescence intensity

The optimum pH conditions for the successful application of the **RhAP** and **RhAP**-Zn^{2+} complex were carefully investigated. For the purpose of this assay, as shown in Fig. 6, the effects of pH on the fluorescence intensity of the **RhAP** chemosensor were measured in the absence and presence of Zn^{2+} in HEPES buffered (10 mM, EtOH:water, 2:1, v/v, pH 7.2). The experiments were conducted at a pH ranging from 4.0 to 11.0. No change in fluorescence intensity was observed in the free chemosensor in an EtOH-water solution when the pH ranged between 7.0 and 11.0. However, small changes in fluorescence intensity were observed under acidic conditions (pH<7). In contrast, the result that occurs when two equivalents of Zn^{2+} are added to a solution of **RhAP**, a red-shifted emission peak at 578 nm was observed in this experiment, with an important enhancement of fluorescence over a comparatively wide pH range (6.0–11). This is due to the spirolactam ring opening as a result of the complexation reaction between the sensor and Zn^{2+}. However, none of the other competing metal ions led to significant changes in fluorescence intensity under identical conditions. In consequence, the results suggest that **RhAP** can be further used as a selective fluorescent turn-on sensor to detect zinc species under physiological pH conditions [16, 18].

Figs. 6

3.4. Determinations of stoichiometry, dissociation constant (K_d) and limit of detection (LOD)

In the proposed system, the stoichiometry of **RhAP**-Zn^{2+} was obtained by using the Job's plot and mole ratio plots methods, as depicted in Fig. 7 and Supplemental Fig. S11 [47]. To determine the dissociation constant of **RhAP**, different amounts of Zn^{2+} ions were titrated into the ethanol-water solution that contained the fluorescent probe. As shown in Supplemental Fig. S9, the addition of various concentrations of Zn^{2+} (ranging from 0–180 μM) changed the emission intensity of **RhAP**. In this titration experiment, a gradual enhancement in the emission intensity of **RhAP** was observed when Zn^{2+} ions were added to the solution [48]. The dissociation constant (K_d) value of Zn^{2+} with **RhAP** was estimated from the emission intensity data following the modified Benesi–Hildebrand equation. [9]. According to the Job's plot assay, assuming a 1:1

binding mode between **RhAP** and Zn^{2+}, the dissociation constant of the **RhAP** chemosensor with zinc ions was determined from the plot of the linear regression of $\log[(F-F_{min})/(F_{max}-F)]$ versus log[M] in equation to find the intercept as 'logK' and the slope as 'n' by using Eq. 1, as follows:

$$\log[(F-F_{min})/(F_{max}-F)] = \log K + n\log[M]$$

Where $\boldsymbol{F}$ is the observed fluorescence and $\boldsymbol{F_{max}}$ is the maximum fluorescence for the **RhAP**-Zn^{2+} complex at an excess amount of zinc ions. $\boldsymbol{F_{min}}$ is the fluorescence of the sensor in absence of Zn^{2+} and '*n*' is the number of Zn^{2+} bound per **RhAP.** [*M*] is the concentration of the zinc ions (μM) added to the **RhAP** solution. Based on the Benesi-Hildebrand equation, the dissociation constant ($\boldsymbol{K_d}$) obtained from the intercept of the linear plot was found to be $\boldsymbol{K_d} = 3.16\text{x}10^{-7}$ M (Fig. 8) [49]. To better demonstrate the selectivity of **RhAP** towards the Zn^{2+} ions, a protocol to determine the LOD was performed using fluorescence titration data with the equation, based on the IUPAC definition ($\text{LOD} = 3S_b/m$), where $\boldsymbol{S_b}$ is the standard deviation of the blank measurements and $\boldsymbol{m}$ is the slope between the fluorescence intensity and the zinc concentrations. Thus, the LOD of **RhAP** with Zn^{2+} was found to be 29 nM, as shown in Fig. 9 [19, 50-51].

Figs. 7, 8 and 9

4. Conclusions

In summary, this paper reports on a rapid and selective fluorescence turn-on detection system for Zn^{2+} based on a rhodamine hydrazone derivative. Overall, the results presented in this study demonstrated that **RhAP** shows highly selective fluorescent enhancement with apparent color change from colorless to purple which provides 'naked-eye' detection of Zn^{2+} ions in an EtOH-water solution. It also found that the fluorescence intensity of **RhAP** at 578 nm displayed a quantitative response to Zn^{2+}. In addition, RhAP exhibited a very low detection limit of 29 nM zinc as compared to sensors that have similar coordination moiety. Based on these findings, **RhAP** is a promising fluorescent probe for detecting Zn^{2+} metal ions in aqueous media under physiological pH conditions. Consequently, the proposed novel **RhAP** might also have a practical application for the selective detection of Zn^{2+} in drinking water and human serums.

Acknowledgements

In this paper, Gaussian 09W used for theoretical calculations was supported by Kilis 7 Aralik University with BAP project 2010/02/08.

References

[1] J. H. Soh, K. M. K. Swamy, S. K. Kim, S. Kim, S. H. Lee, J. Yoon, Rhodamine urea derivatives as fluorescent chemosensors for Hg^{2+} , Tedrahedron Lett. 48(2007) 5966-5969.

[2] D. Lu, L. Yang, Z. Tian, L. Wang, J. Zhang, Core-shell mesoporous silica nanospheres used as Zn^{2+} ratiometric fluorescent sensor and adsorbent, *RSC Advances*, 2(2012) 2783-2789.

[3] H. Xiang Long, L. Yang, L. Tao, Z. Guo Ying, L. Shi Yong, Responsive polymer-based multicolor fluorescent probes for temperature and Zn^{2+} ions in aqueous media, *Sci China Chem*, vol. 57, No. 54, 2014.

[4] D. S. Tira, M. Focsan, S. Ulinici, D. Maniu, S. Astilean, Rhodamine B-Coated Gold Nanoparticles as Effective "Turn-on" Fluorescent Sensors for Detection of Zn II Ions in Water, Spectroscopy letters, 47(2014) 153-159.

[5] J. W. Jeong, B. A. Rao, Y. A. Son, Rhodamine-chloronicotinaldehyde-based "OFF–ON" chemosensor for the colorimetric and fluorescent determination of Al^{3+} ions, Sens. and Actuators B: Chem. 208 (2015) 75–84.

[6] R. Balamurugan, C. C. Chien, K. M. Wu, Y. H. Chiu, J. H. Liu, A depropargylation-triggered fluorescence "turn-on" probe for the detection of Pd2+ based on a bispropargylamine-rhodamine conjugate, Analyst, 138(2013) 1564.

[7] T. Hirayama, K. Okuda, H. Nagasawa, A highly selective turn-on fluorescent probe for iron(II) to visualize labile iron in living cells, Chem. Sci., 4(2013) 1250.

[8] Y. Wei, Z. Aydin, Y. Zhang, Z. Liu, M. Guo, A Turn-on Fluorescent Sensor for Imaging Labile Fe^{3+} in Live Neuronal Cells at Subcellular Resolution, ChemBioChem.13(2012) 1569 – 1573.

[9] L. Zhang, J. Fan, X. Peng, X-ray crystallographic and photophysical properties of rhodamine-based chemosensor for Fe^{3+}, Spectrochim. Acta A 73(2009) 398-402.

[10] R.P. Haugland, 2002, Handbook of Fluorescent Probes and Research Chemicals, 9th ed., Molecular Probes, Eugene, OR.

[11] L. Tang, Y. Li, R. Nandhakumar, J. Qian, An unprecedented rhodamine-based fluorescent and colorimetric chemosensor for Fe^{3+} in aqueous media, Monatsh Chem. 141(2010) 615-620.

[12] J. Ni, Q. Li, B. Li, L. Zhanga, A novel fluorescent probe based on rhodamine B derivative for highly selective and sensitive detection of mercury(II) ion in aqueous, Sens. and Actuators B: Chem. 186 (2013) 278–285.

[13] Y. Hu, J. Zhang, Y. Z. Lv, X. H. Huang, S. l. Hu, A new rhodamine-based colorimetric chemosensor for naked-eye detection of Cu^{2+} in aqueous solution, Spectrochim. Acta A. 157 (2016) 164–169.

[14] J. C. Qin, Z. Y. Yang, G. Q. Wang, A novel ratiometric fluorescent probe for detection of Fe^{3+} by rhodamine–quinoline conjugate, J. Photochem. Photobiol. A Chem. 310 (2015) 122–127.

[15] F. Gea, H. Yea, J. Z. Luo, S. Wang, Y. J. Suna, B. X. Zhao, J. Y. Miao, A new fluorescent and colorimetric chemosensor for Cu(II) based on rhodamine hydrazone and ferrocene unit, Sens. and Actuators B: Chem 181 (2013) 215–220.

[16] V. Dujols, F. Ford, A. W. Czarnik, A Long- Wavelength Fluorescent Chemodosimeter Selective for Cu(II) Ion in Water , J. Am. Chem. Soc. 119(1997) 7386.

[17] L. Fan, J.C. Qin, T.R. Li, B.D Wang, Z.Y. Yang, A novel rhodamine chromen-based "Off-On" chemosensor for the differential detection of Al (III) in aueous solutions, Sens. and Actuators B: Chem. 203(2014) 550-556.

[18] A. Zheng, J. Chen, G. Wu, G. Wu, Y.G. Zhang, A novel fluorescent distinguished probe for Cr(VI) in aqueous solution, Spectrochim. Acta A 74(2009) 265-270.

[19] M. Shellaiah, Y. C. Rajan, P. Balu, A. Murugan, Apyrene based Schiff base probe for selective fluorescence turn-on detection of Hg^{2+} ions with live cell application, New J. Chem. 39(2015) 2523-2531.

[20] M. P. Walkees, Cadmium carcinogenesis, Mutat. Res., 533(2003) 107-120.

[21] M. Waisberg, P. Joseph, B. Hale, D. Beyersmann, Molecular and cellular mechanisms of cadmium carcinogenesis, Toxicology., 192(2003) 95-117.

[22] L. Tang, X. Dai, X. Wen, D. Wu, Q. Zhang, A rhodamine–benzothiazole conjugated sensor for colorimetric, ratiometric and sequential recognition of copper(II) and sulfide in aqueous media, Spectrochim. Acta A 139 (2015) 329–334.

[23] L. Q. Li, L. P. Meng, Novel rhodamine derivate as high selective detection lead sensor, Spectrochim. Acta A 122 (2014) 772–775.

[24] K. Wechakorn, K. Suksen, P. Piyachaturawat , P. Kongsaereea, Rhodamine-based fluorescent and colorimetric sensor for zinc and its application in bioimaging, Sens. and Actuators B: Chem. 228 (2016) 270–277.

[25] B. Zhanga, Q. Diao, P. Maa, X. Liua, D. Songa, X. Wanga, A sensitive fluorescent probe for Cu2+ based on rhodamine B derivatives and its application to drinking water examination and living cells imaging, Sens. and Actuators B: Chem. 225 (2016) 579–585.

[26] A. Raia , N. Kumaria , A. K. Srivastavaa , S. K. Singhb , S. Srikrishnab , L. Mishraa, Rhodamine hydrazone as OFF–ON–OFF type selective sequential sensor of Al^{3+} and N_3- ions, J. Photochem. Photobiol. A Chem. 319 (2016) 78–86.

[27] Q. Diao, P. Ma, L. Lv, T. Li, X. Wang, D. Song, A novel fluorescent probe for Cr^{3+} based on rhodamine–crown ether conjugate and its application to drinking water examination and bioimaging, Spectrochim. Acta A 156 (2016) 15–21.

[28] Q. Huang, Q. Zhang, E. Wang, Y. Zhou, H. Qiao, L. Pang, F. Yu, A new ''off–on'' fluorescent probe for Al^{3+} in aqueous solution based on rhodamine B and its application to bioimaging, Spectrochim. Acta A 152 (2016) 70–76.

[29] J. Xu, Y. Hou, Q. Ma, X. Wu, S. Feng, J. Zhang, Y. Shen, A highly selective fluorescent probe for Cu^{2+} based on rhodamine B derivative, Spectrochim. Acta A 124 (2014) 416–422.

[30] Z. Dong, X. Tian, Y. Chen, J. Hou, Y. Guo, J. Sun, J. Ma, A highly selective fluorescent chemosensor for Hg^{2+} based on rhodamine B and its application as a molecular logic gate, Dyes Pigm 97 (2013) 324-329.

[31] F. Yan, T. Zheng, D. Shi, Y. Zou, Y. Wang, M. Fu, L. Chen, W. Fu, Rhodamine-aminopyridine based fluorescent sensors for Fe^{3+} in water: Synthesis, quantum chemical interpretation and living cell application, Sens. and Actuators B: Chem. 215 (2015) 598–606.

[32] R. Bhowmick, R. Alam, T. Mistri, D. Bhattacharya, P. Karmakar, M. Ali, Morphology-Directing Synthesis of Rhodamine-Based Fluorophore Microstructures and Application toward Extra- and Intracellular Detection of Hg^{2+}, ACS Appl. Mater. Interfaces 7(2015) 7476−7485.

[33] J. Zhang, Y. Zhou, W. Hu, L. Zhang, Q. Huang, T. Ma, Highly selective fluorescence enhancement chemosensor for Hg^{2+} based on rhodamine and its application in living cells and aqueous media, Sens. and Actuators B: Chem. 183 (2013) 290–296.

[34] Y. Jiao, L. Zhang, P. Zhou, A rhodamine B-based fluorescent sensor toward highly selective mercury (II) ions detection, Talanta 150 (2016) 14–19.

[35] X. Chen, X. Meng, S. Wang, Y. Cai, Y. Wu, Y. Feng, M. Zhu, Q. Guo, A rhodamine-based fluorescent probe for detecting Hg^{2+} in a fully aqueous environment, Dalton Trans. 42(2013) 14819-14825.

[36] K. Ghosh, T. Sarkar, A. Majumdar, Rhodamine-labelled new architecture for dual sensing of Co^{2+} and Hg^{2+} ions, Tetrahedron Lett. 54 (2013) 6464–6468.

[37] H. Sasaki, K. Hanaoka, Y. Urano, T. Terai, T. Nagano, Design and synthesis of a novel fluorescence probe for Zn^{2+} based on the spirolactam ring-opening process of rhodamine derivatives, Bioorg. Med. Chem. 19(2011) 1072-1078.

[38] P. Puangploy, S. Smanmoo, W. Surareungchai, A new rhodamine derivative-based chemosensor for highly selective and sensitive determination of Cu^{2+}, Sens. and Actuators B: Chem. 193(2014) 679-686.

[39] M. Wang, F. Yan, Y. Zou, L. Chen, N. Yang, X. Zhou, Recognition of Cu^{2+} and Hg^{2+} in physiological conditions by a new rhodamine based dual channel fluorescent probe, Sens. and Actuators B: Chem. 192(2014) 512-521.

[40] J. Hu, Z. Hu, Y. Cui, X. Zhang, H.W Gao, K. Uvdal, A rhodamine-based fluorescent probe for Hg^{2+} and its application for biological visualization, Sens. and Actuators B: Chem. 203(2014) 452-458.

[41] S. K. Kempahanumakkagari, R. Thippeswamy, P. Malingappa, A new rhodamine B based fluorometric chemodosimeter for Cu^{2+} ion in aqueous and cellular media, J. Lumin. 146 (2014) 11-17.

[42] M. Saleem, Ki. H. Lee, Selective fluorescence detection of Cu^{2+} in aqueous solution and living cells, J. Lumin. 145 (2014) 843-848.

[43] J. H. Chang, Y. M. Choi, Y. K. Shin, A significant fluorescence quenching of anthrylaminobenzocrown ethers by paramagnetic metal cations, Bull. Korean Chem. Soc. 2001, vol, 22, no. 5.

[44] C. Chen, G. Men, W. Bu, C. Liang, H. Sun, S. Jiang, A colorimetric and fluorescent probe for multiple transition metal ions (Cu^{2+}, Zn^{2+}, and Ni^{2+}): fast response and high selectivity, Sens. and Actuators B: Chem. 220(2015) 463-471.

[45] K. Rurack, Flipping the light switch 'ON'-the design of sensor molecules that show cation-induced fluorescence enhancement with heavy and transition metal ions, Spectrochim. Acta A. 57 (2001) 2161-2195.

[46] J. Zhang, L. Zhang, Y. Zhou , T. Ma, J. Niu, A highly selective fluorescent probe for the detection of palladium(II) ion in cells and aqueous media, Microchim Acta 180(2013)211-217.

[47] B. Valeur, S. Berberan, N. Mário, , Molecular Fluorescence: Princeples and Applications, 2. Edition, 2002, Wiley-VCH. Weinheim.

[48] J.T. Hou, Q.F. Zhang, B.Y. Xu, Q. Liu, J. Zhang, X. Q. Yu, A novel BINOL-based cyclophane via click chemistry: synthesis and its applications for sensing silver ions, Tedrahedron Lett. 52(2011) 4927-4930.

[49] X. Y. Liu, D. Y. Liu, J. Qi, Z. G. Cui, H. X. Chang, H. R. He, G. M. Yang, A new fluorescent sensor for Cd^{2+} and its application in living cells imaging, Tetrahedron Lett. 56 (2015) 1322-1327.

[50] Y. Sun, S. Fan, D. Zhao, L. Duan, A Fluorescent Turn-On Probe Based on Benzo [E] Indolium for Cyanide Ion in Water With High Selectivity, J Fluoresc 23(2013) 1255-1261.

[51] K. C. Tayade, A. S. Kuwar, U. A. Fegade, H. Sharma, N. Singh, U. D. Patil, S. B. Atarde, Dessign and Synthesis of a Pyridine Based Chemosensor: Highly Selective Fluorescent Probe For Pb^{2+}, J Fluoresc 24(2014) 19-26.

Figures

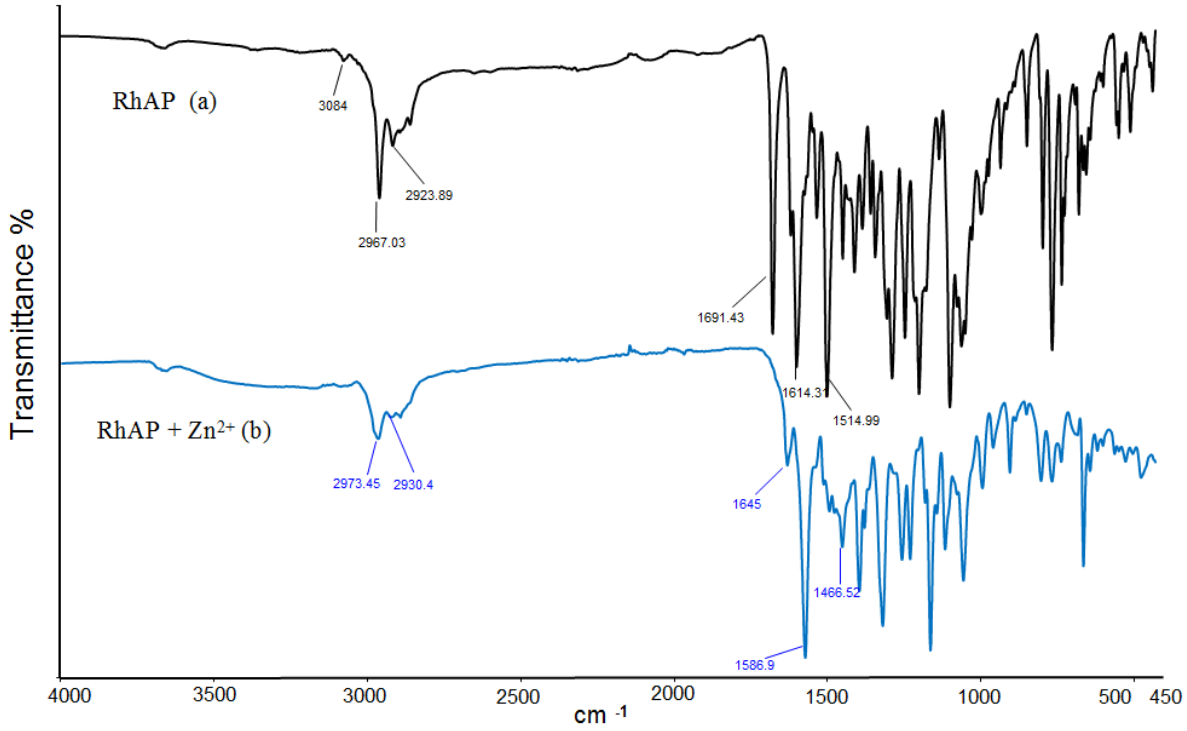

Fig.1. IR spectra shows that **RhAP** before (a) and after (b) addition of Zn^{2+}

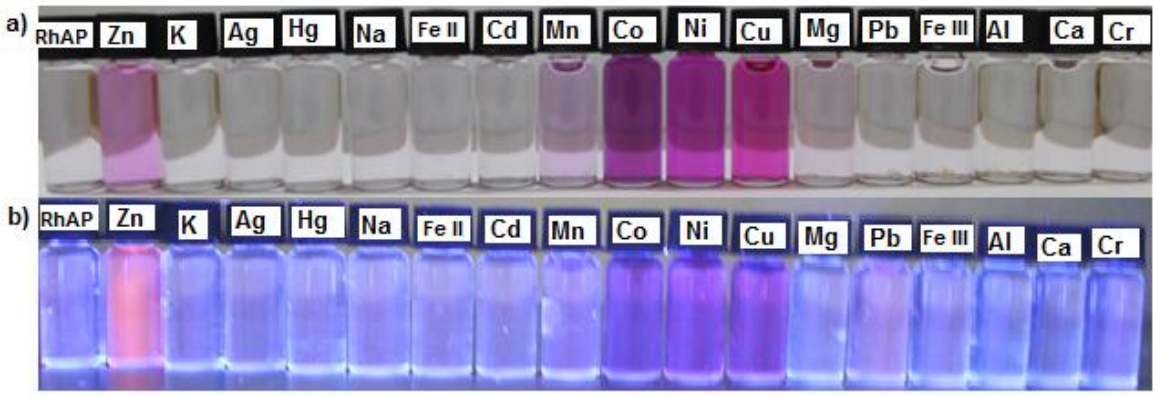

Fig.2. Color changes of **RhAP** (50 µM) in absence and presence of Na^{1+}, K^{1+}, Mg^{2+}, Ca^{2+}, Al^{3+}, Ag^{1+}, Zn^{2+}, Hg^{2+}, Fe^{2+}, Cd^{2+}, Mn^{2+}, Ni^{2+}, Cu^{2+}, Fe^{3+}, Cr^{3+}, Pb^{2+}, Co^{2+} (100 µM) in HEPES buffered (10 mM, EtOH:water, 2:1, v/v, pH 7.2) under visible light (a) and UV lamp at 365 nm (b).

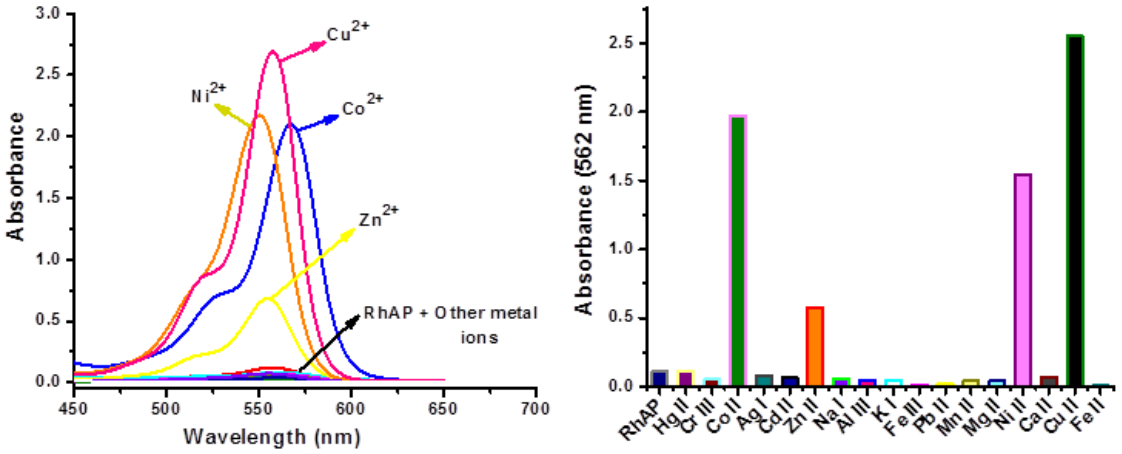

Fig.3. UV-vis spectra of **RhAP** (50 µM) in HEPES buffered (10 mM, EtOH:water, 2:1, v/v, pH 7.2) with 2 equiv. of metal ions: Na^{1+}, K^{1+}, Mg^{2+}, Ca^{2+}, Al^{3+}, Ag^{1+}, Zn^{2+}, Hg^{2+}, Fe^{2+}, Cd^{2+}, Mn^{2+}, Ni^{2+}, Cu^{2+}, Fe^{3+}, Cr^{3+}, Pb^{2+} and Co^{2+} . The bar graph shows the changes of relative absorbance value upon treatment with same metal ions at 562 nm.

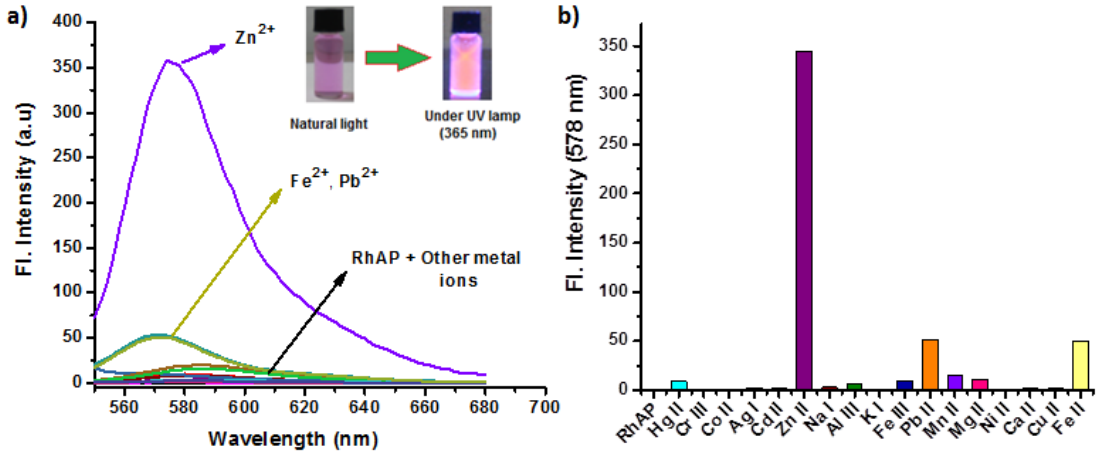

Fig.4. Fluorescence emission spectra of **RhAP** (50 µM) in HEPES buffered (10 mM, EtOH:water, 2:1, v/v, pH 7.2) with 2 equiv. of metal ions: Na^{1+}, K^{1+}, Mg^{2+}, Ca^{2+}, Al^{3+}, Ag^{1+}, Zn^{2+}, Hg^{2+}, Fe^{2+}, Cd^{2+}, Mn^{2+}, Ni^{2+}, Cu^{2+}, Fe^{3+}, Cr^{3+}, Pb^{2+} and Co^{2+}; Insert: Photo picture under visible light and portable UV lamp at 365 nm (a), bar graph representing the changes of relative emission intensity of **RhAP** at 578 nm upon treatment with same metal ions (λ_{ex} = 535 nm) (b).

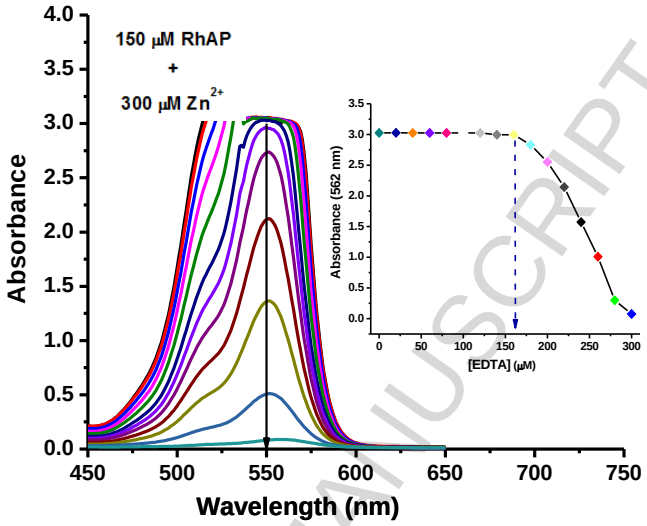

Fig.5. UV-vis spectra changes of **RhAP**+Zn^{2+} with increasing concentration of EDTA (2 equiv., 0 to 300 µM, from top to bottom) in HEPES buffered (10 mM, EtOH:water, 2:1, v/v, pH 7.2). The inset exhibits the absorbance at 562 nm as a function of EDTA concentration.

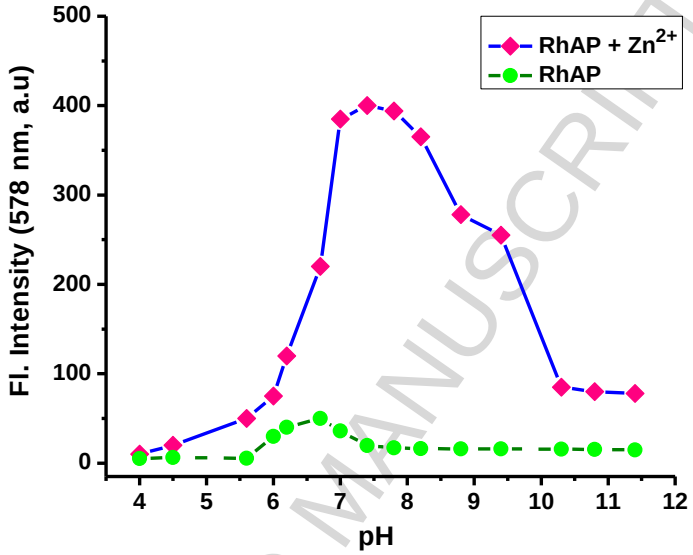

Fig.6. The effect of pH (4.0-11.5) on the relative fluorescence intensity of **RhAP (**50 µM) in the absence (●) and presence (◆) of Zn^{2+} (1 equiv.) in HEPES buffered (10 mM, EtOH:water, 2:1, v/v, pH 7.2). The pH values of solution were adjusted by using an appropriate volume of 0.1 M HCl or NaOH stock solution.

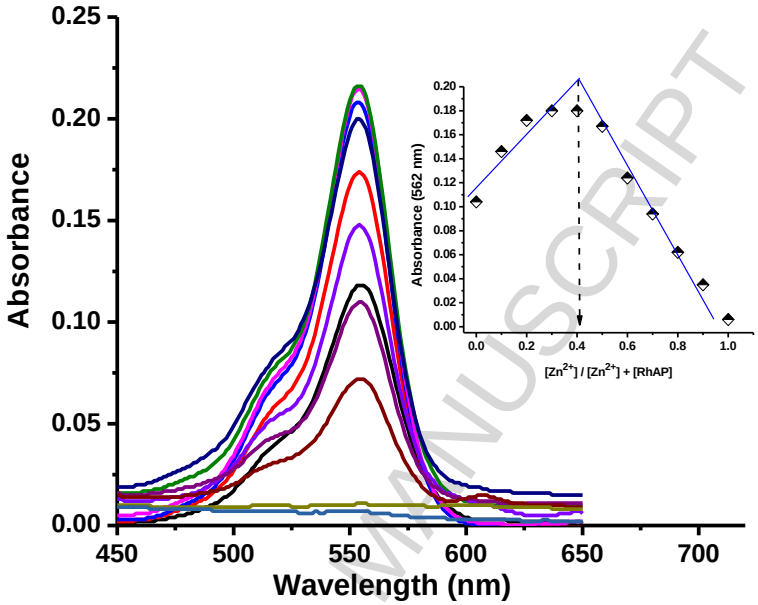

Fig.7. Job's plot established from the absorption spectra of **RhAP** and Zn^{2+} under a constant total concentration. The inset shows the absorbance at 562 nm as a function of {[Zn^{2+}]/[Zn^{2+}]+[**RhAP**]} value.

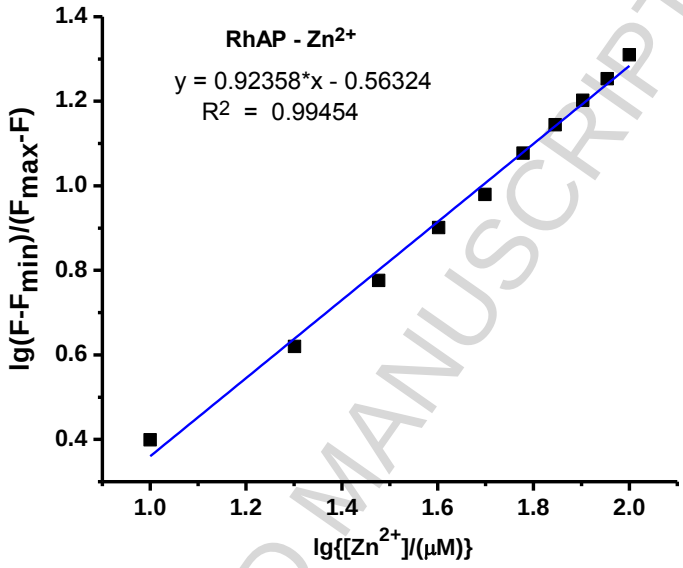

Fig.8. Benesi-Hildebrand plot (fluorescence intensity at 578 nm, λ_{ex} = 535 nm) of **RhAP**, assuming a 1:1 binding mode for association between **RhAP** and Zn^{2+}.

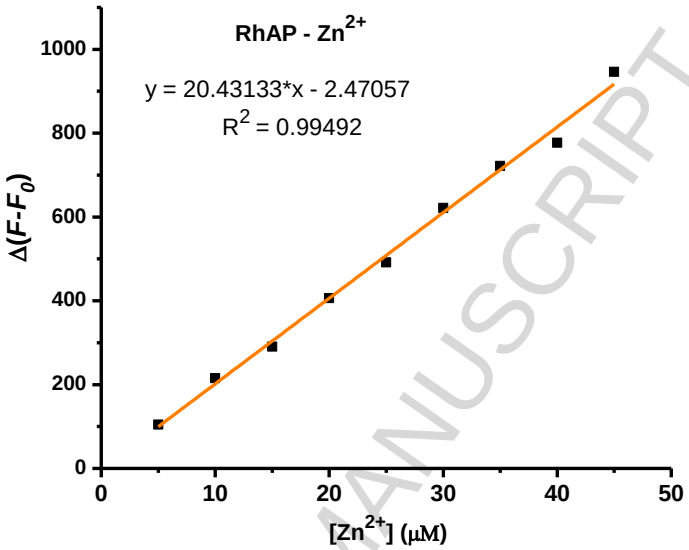

Fig.9. Fluorescence intensity at 578 nm of **RhAP** upon continuous addition of increasing amount of Zn^{2+} (0-50 μM) in HEPES buffered (10 mM, EtOH:water, 2:1, v/v, pH 7.2, λ_{ex} = 535 nm).

Graphical Abstract

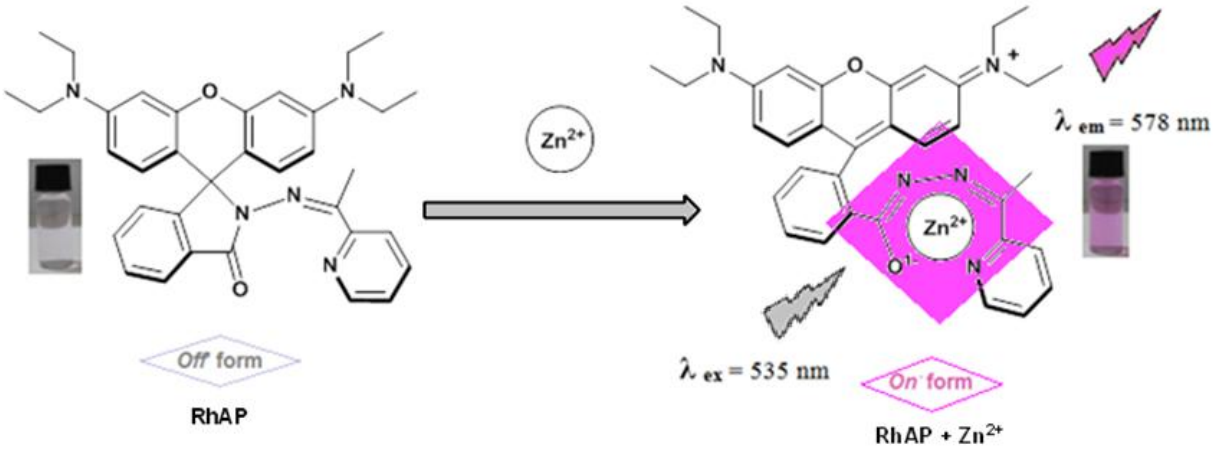

Proposed binding mode of sensor **RhAP** and Zn^{2+} in EtOH-water (2:1, v/v) solution

Highlights

- Synthesis and characterization of a new fluorescent sensor '**RhAP**'
- The selectivity of **RhAP** for Zn^{2+} was investigated by spectroscopic techniques
- The results showed that the sensor may be further performed for the selective detection of Zn^{2+} in aqueous media